

Effective mass enhancement of two-dimensional electrons in a one-dimensional superlattice potential

Amlan Majumdar,^{a)} L. P. Rokhinson, and D. C. Tsui

Department of Electrical Engineering, Princeton University, Princeton, New Jersey 08544

L. N. Pfeiffer and K. W. West

Bell Laboratories, Lucent Technologies, Murray Hill, New Jersey 07974

(Received 7 October 1999; accepted for publication 11 April 2000)

We report effective mass enhancement of two-dimensional (2D) electrons in an atomically precise one-dimensional AlGaAs/GaAs superlattice potential fabricated by the cleaved-edge overgrowth technique. Magnetotransport measurements reveal that the mobility of the 2D electrons increases with electron density n_{2D} . At low densities ($n_{2D} \sim 1.3 \times 10^{11} \text{ cm}^{-2}$), the effective mass m^* of the 2D electrons is $0.14 m_e$, where m_e is the free-electron mass. This value of $0.14 m_e$ is twice the effective mass of electrons in GaAs ($0.067 m_e$). m^* increases with n_{2D} and is $\sim 0.16 m_e$ at $2.7 \times 10^{11} \text{ cm}^{-2}$. We explain these results based on the formation of energy minibands along the superlattice direction. The electron scattering time τ is calculated from the mobility and effective mass data. At 0.3 K, τ increases with n_{2D} from 5 to 11 ps as n_{2D} is varied from 1.1×10^{11} to $2.7 \times 10^{11} \text{ cm}^{-2}$. © 2000 American Institute of Physics. [S0003-6951(00)03232-4]

Electrons in a periodic potential have an energy band structure that is periodic in k space. In the presence of a constant electric field, the electron k vector increases with time until the edge of the first Brillouin zone (BZ) is reached. At the BZ edge, the k vector suffers Bragg reflection. This causes the electrons to oscillate in real space.^{1,2} Devices based on this phenomenon, called Bloch oscillations (BOs), could be used as high-frequency oscillators. In solids with imperfections, the electrons must be able to reach the BZ edge before being scattered for the observation of BOs. In other words, the electron scattering time τ must be larger than the BO time period $T_B = h/eEd$, where h is the Planck's constant, e is the charge of an electron, E is the constant electric field, and d is the periodicity of the lattice. In 1970, Esaki and Tsu³ suggested the use of semiconductor superlattices (SLs) to look for BOs. They predicted negative differential conductance in these devices when electrons are accelerated to the negative effective mass region of the energy miniband.

After Esaki and Tsu's prediction, a lot of experiments have been done on doped and undoped SL devices. Negative differential velocity has been observed in undoped SLs⁴ and in three-terminal devices where an undoped SL is placed between two of the terminals.⁵ BOs have been observed in optical experiments on undoped SLs.⁶⁻⁸ These undoped SL devices, however, have extremely low electron densities. To use Bloch oscillators as a source of high-frequency radiation, high electron densities are required. In doped SLs, ionized impurity scattering leads to very small τ and the electrons are scattered before they reach the edge of the BZ. The application of high electric fields across doped SLs does lower T_B but causes the formation of high-field domains that lead to nonuniform electric field distribution in the SL.^{9,10} To circumvent all the above-mentioned problems, Stormer *et al.*¹¹

fabricated a lateral SL device using the cleaved-edge overgrowth (CEO) technique.¹² In this device, a two-dimensional electron gas (2DEG) resides in an atomically precise one-dimensional superlattice potential. Kurdak *et al.*¹³ studied high-field transport in these CEO SL devices. They observed nonlinear current-voltage characteristics that were attributed to electron trapping induced by high electric fields.

In this letter, we report ohmic magnetotransport measurements on CEO SL devices with a metal gate. The two-dimensional (2D) electron mobility increases with electron density. At 0.3 K, the mobility changes from 65,000 to 120,000 cm^2/Vs as the density is increased from 1×10^{11} to $2.7 \times 10^{11} \text{ cm}^{-2}$. The temperature dependence of Shubnikov-de Haas (SdH) oscillations in transconductance is used to extract the effective mass of the 2D electrons in the SL. At low electron densities ($\sim 1.3 \times 10^{11} \text{ cm}^{-2}$), the effective mass is $0.14 m_e$, twice that of electrons in GaAs. The effective mass increases from this enhanced value as the 2D electron density increases and is found to be $\sim 0.16 m_e$ at $2.7 \times 10^{11} \text{ cm}^{-2}$, the highest density obtained in our SL device. These observations are explained in terms of energy miniband formation along the SL direction. We calculated the electron scattering time from our mobility and effective mass data. The scattering time increases with 2D electron density. At 0.3 K, it changes from 5 ps at $1.1 \times 10^{11} \text{ cm}^{-2}$ to 11 ps at $2.7 \times 10^{11} \text{ cm}^{-2}$.

The SL device structure is shown in Fig. 1. An undoped SL with heavily doped contact layers is fabricated by the first molecular-beam epitaxy (MBE) growth. A 3000 Å layer of n^+ -GaAs is grown on a (001) GaAs substrate followed by a 350 period compositional SL. The SL consists of 84.9 Å GaAs quantum wells and 28.3 Å $\text{Al}_{0.3}\text{Ga}_{0.7}\text{As}$ barriers. The bottom 100 periods and the top 125 periods of the SL are heavily doped with Si (10^{18} cm^{-3}). The middle 125 periods are undoped. The second MBE growth is performed immediately after cleaving the SL substrate *in situ*. The overgrown

^{a)}Electronic mail: majumdar@ee.princeton.edu

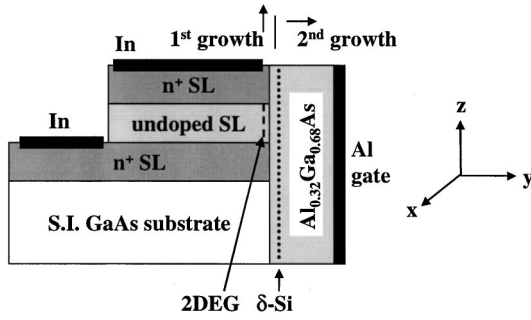


FIG. 1. Schematic cross-sectional diagram of the CEO SL device.

structure on the (110) cleaved-edge facet of the substrate wafer includes a 350 Å spacer layer of undoped $\text{Al}_{0.32}\text{Ga}_{0.68}\text{As}$ followed by 10^{12} cm^{-2} Si δ -doping, a 2000 Å layer of undoped $\text{Al}_{0.32}\text{Ga}_{0.68}\text{As}$, and a 100 Å n^+ -GaAs cap layer. Charge transfer from the Si δ -doping layer gives rise to a 2DEG that resides in the undoped section of the SL. The heavily doped regions of the SL serve as top (drain) and bottom (source) contacts to the 2DEG. $0.5 \text{ mm} \times 1 \text{ mm}$ top contact mesas were defined by wet etching the CEO samples down to the bottom (source) contact layer. Indium contacts were alloyed at 420 °C for 15 s to make shallow ohmic contacts to the source and drain n^+ layers. A 2000 Å thick layer of Al was subsequently evaporated on the cleaved-edge facet to serve as a gate. Gate leakage current is less than 1 nA for gate voltages (V_G) in the range from -1.2 to 0.5 V for temperatures $T < 4.2 \text{ K}$.

We first measured the two-terminal conductance G of the SL device in a perpendicular magnetic field B in a ^3He system at $T=0.3 \text{ K}$ for different gate voltages. Standard lock-in techniques were used for these measurements. The drain-source current $I_{\text{DS}}=500 \text{ nA}$. G as a function of B is shown in Fig. 2 with dotted lines for $V_G=0.0 \text{ V}$ at $T=0.3 \text{ K}$. G decreases with increasing B and the onset of SdH oscillations is observed at $B=0.7 \text{ T}$. At higher temperatures, the onset of SdH oscillations shifts to higher values of B . $n_{2\text{D}}$ is obtained from the period of the SdH oscillations. The gate voltage dependence of $n_{2\text{D}}$ is plotted in the inset of Fig. 2.

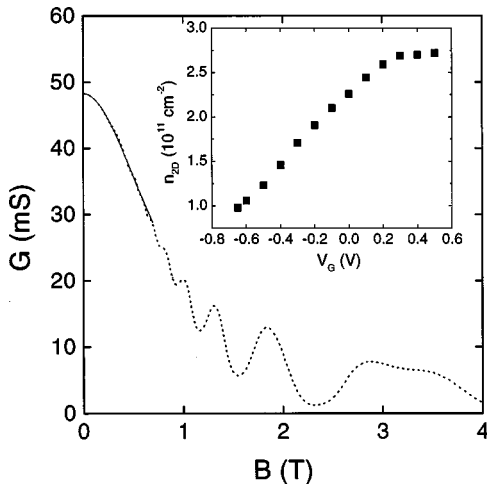


FIG. 2. Conductance of the SL device (dotted line) as a function of magnetic field at $T=0.3 \text{ K}$ for $V_G=0.0 \text{ V}$. $n_{2\text{D}}=2.25 \times 10^{11} \text{ cm}^{-2}$ is obtained from the period of the SdH oscillation. For low B fields, the least-squares fit (solid line) of $G(B)=G_{xx}(B)G_s/(G_{xx}(B)+G_s)$ to the data to obtain μ is shown. Inset: V_G dependence of $n_{2\text{D}}$.

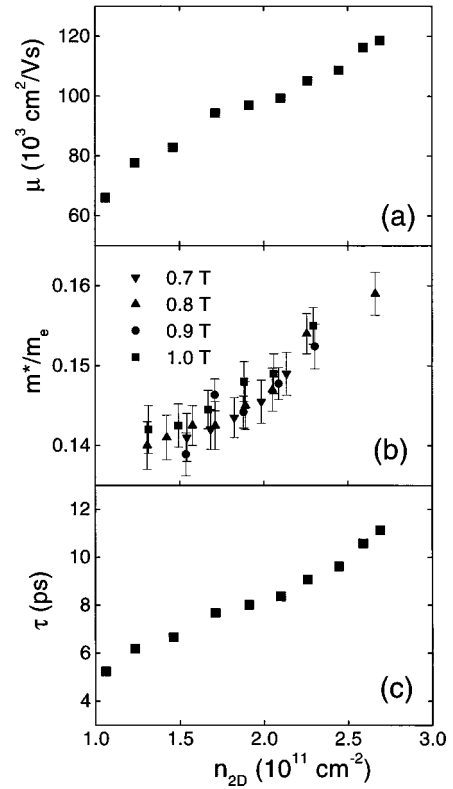


FIG. 3. 2D electron density dependence of (a) mobility at $T=0.3 \text{ K}$, (b) effective mass, and (c) scattering time at $T=0.3 \text{ K}$. The effective mass is extracted from T -dependent SdH oscillations in transconductance at different magnetic fields.

$n_{2\text{D}}$ increases linearly with V_G in the range $-0.65 \text{ V} < V_G < 0.2 \text{ V}$ and then saturates for $V_G > 0.3 \text{ V}$. For $V_G < -0.65 \text{ V}$, we did not observe any SdH oscillations and, hence, could not determine $n_{2\text{D}}$.

The length-to-width aspect ratio of the 2DEG in our sample is approximately 1:1000. This is similar to the Corbino geometry at low B fields.¹¹ Thus, we measure the diagonal conductance (G_{xx}) in series with a conductance G_s coming from the sheet resistance of the source and drain contact layers. For low B fields, $G_{xx}(B)=G_0/(1+\mu^2 B^2)$, where $G_0=(e\mu n_{2\text{D}}W)/L$ is the zero-field conductance, μ is the mobility of the 2DEG, and L and W are the length and width of the 2DEG channel. We fit our data with $G(B)=G_{xx}(B)G_s/(G_{xx}(B)+G_s)$ for $B < 0.6 \text{ T}$ and extract μ . The least-squares fit of $G(B)$ (solid line) to a typical $G-B$ trace (dotted line) is shown in Fig. 2. In Fig. 3(a), we plot μ as a function of $n_{2\text{D}}$ at $T=0.3 \text{ K}$. We see that μ increases with $n_{2\text{D}}$. There is a factor of 2 enhancement in μ from 65,000 to 120,000 $\text{ cm}^2/\text{Vs}$ as $n_{2\text{D}}$ increases from 1×10^{11} to $2.7 \times 10^{11} \text{ cm}^{-2}$.

The effective mass m^* of the 2D electrons can be extracted from the T dependence of the amplitude A of the SdH oscillations:¹⁴

$$A \propto \xi / \sinh(\xi), \quad (1)$$

where $\xi=2\pi^2 k_B T / \hbar \omega_c$, $\omega_c=eB/m^*$ is the cyclotron frequency, k_B is the Boltzmann constant, and $\hbar=h/2\pi$. Although Eq. (1) describes the T dependence of conductivity σ_{xx} derived in Ref. 14, it is also valid for the T dependence of transconductance $G_m=dI_{\text{DS}}/dV_G \propto d\sigma_{xx}/dn_{2\text{D}}$ within 1% for the parameters of our sample. We measured G_m as a

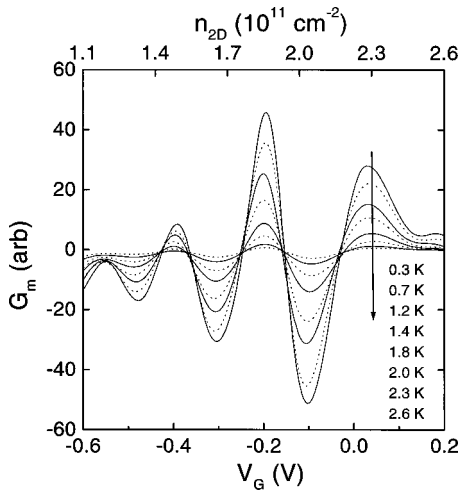


FIG. 4. Transconductance of the SL device as a function of gate voltage for different temperatures at $B = 1$ T.

function of V_G at fixed B -fields at many different temperatures in the range from 0.3 to 4 K. G_m is shown as a function of V_G at $B = 1$ T in Fig. 4 for different temperatures. SdH oscillations in G_m are clearly observed down to $n_{2D} = 1.1 \times 10^{11} \text{ cm}^{-2}$. For each extrema, we fit the T -dependent amplitude of the SdH oscillations to Eq. (1) and determine m^* . In Fig. 3(b), m^* is plotted as a function of n_{2D} for different B -fields. We see that within experimental error m^* is independent of B . At the lowest carrier density $n_{2D} = 1.3 \times 10^{11} \text{ cm}^{-2}$, m^* is $0.14 m_e$. This value of m^* is twice the effective mass of electrons in GaAs ($0.067 m_e$). m^* increases with n_{2D} and reaches $\sim 0.16 m_e$ at $n_{2D} = 2.7 \times 10^{11} \text{ cm}^{-2}$. The scattering time $\tau = \mu m^* / e$ for each n_{2D} is plotted in Fig. 3(c). τ increases with n_{2D} from 5 ps at $1.1 \times 10^{11} \text{ cm}^{-2}$ to 11 ps at $2.7 \times 10^{11} \text{ cm}^{-2}$. τ increases faster than m^* as a function of n_{2D} . This is why we observe a significant increase in μ with n_{2D} .

The 15% increase in m^* with increasing n_{2D} is a SL effect. Effective mass is inversely proportional to the curvature of the energy dispersion relation. For the energy dispersion along the SL direction, the curvature is positive for low energies and negative for high energies. The curvature goes to zero somewhere near the middle of the energy miniband. Therefore, m^* increases with energy and diverges near the middle of the miniband. For our 2D system, the electrons experience the SL potential along the z direction. However, the electrons are free to move along the x direction (see Fig.

1). Thus, the electrons have parabolic energy dispersion and constant effective mass along x . The effective mass we measure using B -fields is the cyclotron effective mass. It is a combination of the energy dependent m^* along the z direction and the constant m^* along the x direction. It increases with energy and diverges only near the top of the energy miniband. As we increase the 2D electron density, we sweep the Fermi energy through the energy miniband and, hence, observe increasing electron effective mass. This observation is, therefore, consistent with the formation of energy minibands along the SL direction.

In conclusion, we have investigated the energy band structure of 2D electrons in a periodic potential by measuring their effective mass. At low electron densities ($n_{2D} \sim 1.3 \times 10^{11} \text{ cm}^{-2}$), the effective mass $m^* = 0.14 m_e$, where m_e is the free-electron mass. This value of $0.14 m_e$ is twice the m^* of electrons in GaAs ($0.067 m_e$). m^* increases with n_{2D} and is $\sim 0.16 m_e$ at $2.7 \times 10^{11} \text{ cm}^{-2}$. We have also observed that at 0.3 K, both the mobility and scattering time of the 2D electrons increase, by a factor of 2, with n_{2D} in the density range we were able to probe in our CEO SL device.

The authors wish to thank Y. H. Chang, M. Grayson, M. Hilke, C. Li, and J. Yoon for their help and useful discussions. The work at Princeton University is supported by the ARO.

¹F. Bloch, Z. Phys. **52**, 555 (1928).

²C. Zener, Proc. R. Soc. London, Ser. A **145**, 523 (1934).

³L. Esaki and R. Tsu, IBM J. Res. Dev. **14**, 61 (1970).

⁴A. Sibille, J. F. Palmier, C. Minot, and F. Mollot, Appl. Phys. Lett. **54**, 165 (1989).

⁵F. Beltram, F. Capasso, D. L. Sivco, A. L. Hutchinson, S.-N. G. Chu, and A. Y. Cho, Phys. Rev. Lett. **64**, 3167 (1990).

⁶J. Feldmann, K. Leo, J. Shah, D. A. B. Miller, J. E. Cunningham, T. Meier, G. von Plessen, A. Schulze, P. Thomas, and S. Schmitt-Rink, Phys. Rev. B **46**, 7252 (1992).

⁷C. Waschke, H. G. Roskos, R. Schwedler, K. Leo, H. Kurz, and K. Kohler, Phys. Rev. Lett. **70**, 3319 (1993).

⁸T. Dekorsy, P. Leisching, K. Kohler, and H. Kurz, Phys. Rev. B **50**, 8106 (1994).

⁹L. Easki and L. L. Chang, Phys. Rev. Lett. **33**, 495 (1974).

¹⁰K. K. Choi, B. F. Levine, R. J. Malik, J. Walker, and C. G. Bethea, Phys. Rev. B **35**, 4172 (1987).

¹¹H. L. Stormer, L. N. Pfeiffer, K. W. Baldwin, K. W. West, and J. Spector, Appl. Phys. Lett. **58**, 726 (1991).

¹²L. N. Pfeiffer, K. W. West, H. L. Stormer, J. P. Eisenstein, K. W. Baldwin, D. Gershoni, and J. Spector, Appl. Phys. Lett. **56**, 1697 (1990).

¹³C. Kurdak, A. Zaslavsky, D. C. Tsui, M. B. Santos, and M. Shayegan, Appl. Phys. Lett. **66**, 323 (1995).

¹⁴T. Ando, A. B. Fowler, and F. Stern, Rev. Mod. Phys. **54**, 437 (1982).